NATIONAL ADVISORY COMMITTEE FOR AERONAUTICS

REPORT 1023

DIFFUSION OF CHROMIUM IN ALPHA COBALT-CHROMIUM SOLID SOLUTIONS

By JOHN W. WEETON

1951

For sale by the Superintendent of Documents, U. S. Government Printing Office, Washington 25, D. C. Yearly subscription, $4; foreign, $5.25; single copy price varies according to size. - - - - - - - - - Price 20 cents

AERONAUTIC SYMBOLS

1. FUNDAMENTAL AND DERIVED UNITS

	Symbol	Metric		English	
		Unit	Abbreviation	Unit	Abbreviation
Length	l	meter	m	foot (or mile)	ft (or mi)
Time	t	second	s	second (or hour)	sec (or hr)
Force	F	weight of 1 kilogram	kg	weight of 1 pound	lb
Power	P	horsepower (metric)		horsepower	hp
Speed	V	kilometers per hour	kph	miles per hour	mph
		meters per second	mps	feet per second	fps

2. GENERAL SYMBOLS

W Weight$=mg$

g Standard acceleration of gravity$=9.80665$ m/s^2 or 32.1740 ft/sec^2

m Mass$=\frac{W}{g}$

I Moment of inertia$=mk^2$. (Indicate axis of radius of gyration k by proper subscript.)

μ Coefficient of viscosity

ν Kinematic viscosity

ρ Density (mass per unit volume)

Standard density of dry air, 0.12497 kg-m^{-4}-s^2 at 15° C and 760 mm; or 0.002378 lb-ft^{-4} sec^2

Specific weight of "standard" air, 1.2255 kg/m^3 or 0.07651 lb/cu ft

3. AERODYNAMIC SYMBOLS

S Area

S_w Area of wing

G Gap

b Span

c Chord

A Aspect ratio, $\frac{b^2}{S}$

V True air speed

q Dynamic pressure, $\frac{1}{2}\rho V^2$

L Lift, absolute coefficient $C_L=\frac{L}{qS}$

D Drag, absolute coefficient $C_D=\frac{D}{qS}$

D_0 Profile drag, absolute coefficient $C_{D_0}=\frac{D_0}{qS}$

D_i Induced drag, absolute coefficient $C_{D_i}=\frac{D_i}{qS}$

D_p Parasite drag, absolute coefficient $C_{D_p}=\frac{D_p}{qS}$

C Cross-wind force, absolute coefficient $C_C=\frac{C}{qS}$

i_w Angle of setting of wings (relative to thrust line)

i_t Angle of stabilizer setting (relative to thrust line)

Q Resultant moment

Ω Resultant angular velocity

R Reynolds number, $\rho\frac{Vl}{\mu}$ where l is a linear dimension (e.g., for an airfoil of 1.0 ft chord, 100 mph, standard pressure at 15° C, the corresponding Reynolds number is 935,400; or for an airfoil of 1.0 m chord, 100 mps, the corresponding Reynolds number is 6,865,000)

α Angle of attack

ϵ Angle of downwash

α_0 Angle of attack, infinite aspect ratio

α_i Angle of attack, induced

α_a Angle of attack, absolute (measured from zero-lift position)

γ Flight-path angle

REPORT 1023

DIFFUSION OF CHROMIUM IN ALPHA COBALT-CHROMIUM SOLID SOLUTIONS

By JOHN W. WEETON

Lewis Flight Propulsion Laboratory
Cleveland, Ohio

National Advisory Committee for Aeronautics

Headquarters, 1724 F Street NW, Washington 25, D. C.

Created by act of Congress approved March 3, 1915, for the supervision and direction of the scientific study of the problems of flight (U. S. Code, title 50, sec. 151). Its membership was increased from 12 to 15 by act approved March 2, 1929, and to 17 by act approved May 25, 1948. The members are appointed by the President, and serve as such without compensation.

TECHNICAL COMMITTEES

AERODYNAMICS
POWER PLANTS FOR AIRCRAFT
AIRCRAFT CONSTRUCTION
OPERATING PROBLEMS
INDUSTRY CONSULTING

Coordination of Research Needs of Military and Civil Aviation
Preparation of Research Programs
Allocation of Problems
Prevention of Duplication
Consideration of Inventions

LANGLEY AERONAUTICAL LABORATORY, Langley Field, Va.

LEWIS FLIGHT PROPULSION LABORATORY, Cleveland Airport, Cleveland, Ohio

AMES AERONAUTICAL LABORATORY Moffett Field, Calif.

Conduct, under unified control, for all agencies, of scientific research on the fundamental problems of flight

---

OFFICE OF AERONAUTICAL INTELLIGENCE,
Washington, D. C.

Collection, classification, compilation, and dissemination of scientific and technical information on aeronautics

REPORT 1023

DIFFUSION OF CHROMIUM IN ALPHA COBALT-CHROMIUM SOLID SOLUTIONS [1]

by JOHN W. WEETON

SUMMARY

Diffusion of chromium in α cobalt-chromium solid solutions was investigated in the range 0 to 40 atomic percent at temperatures of 1360°, 1300°, 1150°, and 1000° C. The diffusion coefficients were found to be relatively constant within the composition range covered by each specimen.

The activation heat of diffusion was determined to be 63,600 calories per mole. This value agrees closely with the value of 63,400 calories per mole calculated by means of the Dushman-Langmuir equation. The exponential equation relating diffusion coefficient D to temperature T is as follows:

$$D = 0.443e^{-\frac{63{,}600}{RT}}$$

where R is the gas constant.

When compared with the diffusion data previously obtained by other investigators for most alloy systems, the diffusion rates of chromium in α cobalt-chromium were found to be low; considerably higher temperatures were required to produce diffusion coefficients of the same order of magnitude as were previously found for most substitutional alloys. This behavior is congruous with the fact that cobalt-chromium based alloys such as Haynes Stellite 21 have good high-temperature characteristics.

Chromium diffusivity from α cobalt-chromium alloys into pure cobalt is greater than chromium diffusivity from high-chromium α-alloys to low-chromium α-alloys for all concentration gradients studied.

INTRODUCTION

Several important high-temperature alloys (Haynes Stellite 21, X-40, 61, and 422-19) consist primarily of cobalt and chromium; Haynes Stellite 21 has been one of the most extensively used turbojet-blade alloys in the United States. Because of the importance of cobalt-chromium based alloys and because diffusion controls many reactions within solid metals, an investigation was conducted at the NACA Lewis laboratory to determine the diffusion coefficients of chromium into α cobalt-chromium solid solutions, to determine the dependence of these coefficients on concentration, and to evaluate the basic constants Q and A in the exponential equation relating temperature and diffusion (reference 1)

$$D = Ae^{-\frac{Q}{RT}}$$

where

A constant, (cm²/sec)
D diffusion coefficient, (cm²/sec)
Q activation heat of diffusion, (cal/mole)
R gas constant, (cal/(mole) (°K))
T temperature, (°K)

The method employed consisted in pressure-welding cobalt and cobalt-chromium bars unlike in composition, annealing these joined bars at constant temperatures to cause an interdiffusion of atoms, and determining the distribution of chromium through the diffusion zones thus formed by machining and chemically analyzing several successive turnings through this zone.

Diffusion coefficients were determined for 11 specimens at the nominal temperatures and composition ranges shown in the following table:

CHROMIUM CONTENT OF WELDED SPECIMENS (ATOMIC PERCENT)

1360° C			1300° C			1150° C			1000° C		
	Composition			Composition			Composition			Composition	
Specimen	Low-Cr half	High-Cr half	Specimen	Low-Cr half	High-Cr half	Specimen	Low-Cr half	High-Cr half	Specimen	Low-Cr half	High-Cr half
1	0	22.20	3	0	28.00	6	13.15	38.65	8	0	24.92
2	9.60	28.06	4	9.60	41.15	7	0	28.06	9	9.80	39.97
11	0	28.00	5	9.98	39.20						
			10	0	28.15						

With the exception of specimens 1 and 2, which were originally intended for annealing at 900° C, the specimens were made to cover most of the range of the α field in the cobalt-chromium equilibrium diagram (fig. 1).

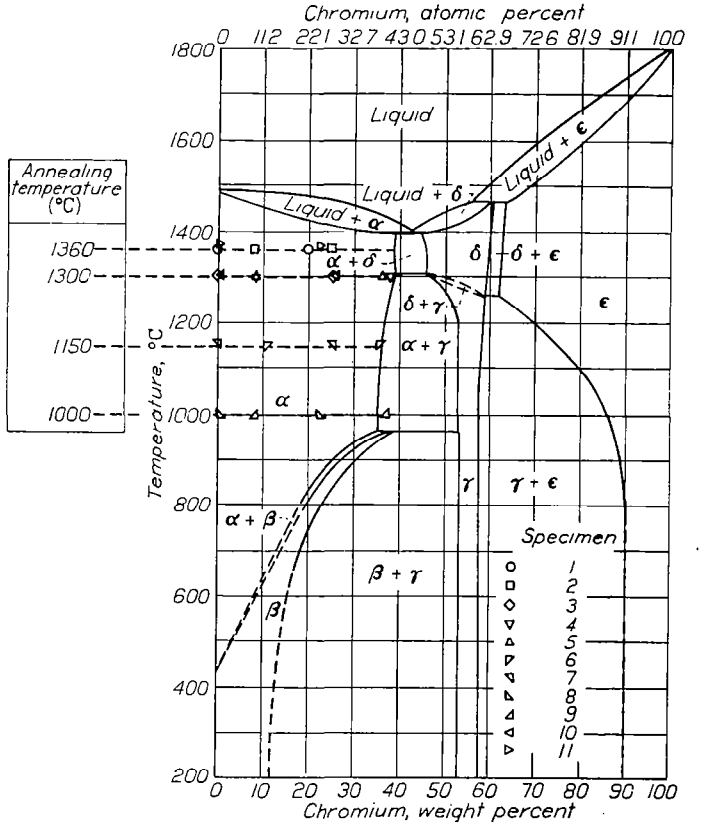

FIGURE 1. – Cobalt-chromium equilibrium diagram from reference 2. Also drawn are composition ranges at annealing temperatures used in this investigation.

[1] Supersedes NACA TN 2218, "Diffusion of Chromium in α Cobalt-Chromium Solid Solutions" by John W. Weeton, 1950.

960191—51

Diffusion coefficients were calculated by the Grube method (reference 3), although the Matano method (reference 3) was also used in two cases.

APPARATUS AND PROCEDURE

Materials.—Cobalt rondels and electrolytic chromium of high purity were used as raw materials. Spectrographic and wet chemical analyses were made of the rondels. Colorimetric analyses, made for elements that were shown to be present by the spectrograph but were not detectable by wet chemical methods, are less than 0.01 percent. The results of the analysis of cobalt rondels and of an analysis of electrolytic chromium made by the supplier, the Bureau of Mines, are given in the following table:

IMPURITIES IN COBALT AND CHROMIUM

Cobalt rondels (percent)			Electrolytic chromium (percent)	
Ni		0.38	Fe	0.31
Fe		.10	O	.17
Cu		.08		
Mn	<	.01		
Sn	<	.01		
Ag	<	.01		
Pb	<	.01		
Ti	<	.01		
V	<	.01		
C		[a].14,.20		

[a] Determined by commercial laboratory.

It will be shown that the carbon content was considerably reduced during melting.

Melting and casting.—Cobalt and cobalt-chromium melts of nominally 0, 10, 25, and 35 percent-by-weight chromium (0, 11, 27, and 38 atomic percent) were made in zirconium silicate crucibles, using a 100-kilowatt, 9600-cycle-per-second induction unit. The rondels were first melted with no protective atmosphere and were held at temperatures of 1593° to 1649° C (2900° to 3000° F) for 5 to 10 minutes to burn out the carbon. As a result of this procedure, the carbon was reduced to less than 0.06 percent in most cases, but the oxide content of the metal was probably increased.

Where chromium additions were required, an atmosphere of argon was kept over the surface of the melt from the time the addition was made until the pouring time, a total period of 10 to 20 minutes. Chromium was not charged with the cobalt because chromium prevents oxidation and removal of almost all the carbon.

Castings were made in copper molds and, except for the heads, were shaped like truncated cones 4 inches long, 1¼ inches in diameter at the top, and ⅞ inch in diameter at the bottom. Chemical analyses made from both ends of the castings containing chromium indicated that the churning action of the induction current produced an excellent degree of chemical homogeneity; differences in chromium analyses made from the large and the small ends of castings ranged from 0.02 to 0.15 percent.

Heat treatment prior to forging.—As a precautionary measure, the samples containing chromium were soaked at 1176° to 1231° C (2150° to 2250° F) for ½ hour and then oil-quenched. This treatment was intended to reduce the possibility of cracking the samples if insufficient soaking time were allowed prior to forging.

Forging.—The tapered castings, which were forged at a commercial laboratory, were upset one or two times and were fullered out to an approximately uniform diameter of 1 inch. The reduction in length occurring when the castings were upset varied from approximately 20 to 50 percent. Forging at temperatures from 982° to 1093° C (1800° to 1900° F) reduced the grain size from grains as large as ¼ inch to smaller, more uniformly shaped grains that varied from A. S. T. M. grain size 5 to small macroscopic grains approximately 1/64 inch.

Homogenizing heat-treatment.—The samples containing chromium were annealed at 1204° C (2200° F) for 3 hours in a helium atmosphere for further homogenization. Results presented herein indicate that this treatment does little more than stress-relieve the specimens.

Machining of bars to be welded.—Cylinders ⅞ inch in diameter and 1¾ to 2¼ inches in length were machined from the forged bars. Both ends of these cylinders were surface ground to produce flatness and one end of each bar was then lapped by a gage-block manufacturer until it could be "wrung" to another bar.

Welding of dissimilar bars or cylinders.—Lapped specimens of unlike compositions were placed in the holders shown in figure 2. The upper holder was bolted to a 120,000-pound tensile machine and the lower one was placed on the table of the machine. A load of 5000 pounds was applied after the cylinders were centered in an induction coil and the holders were alined. The specimens were heated with a portable, 35-kilowatt, 360,000-cycle-per-second, spark-gap induction unit.

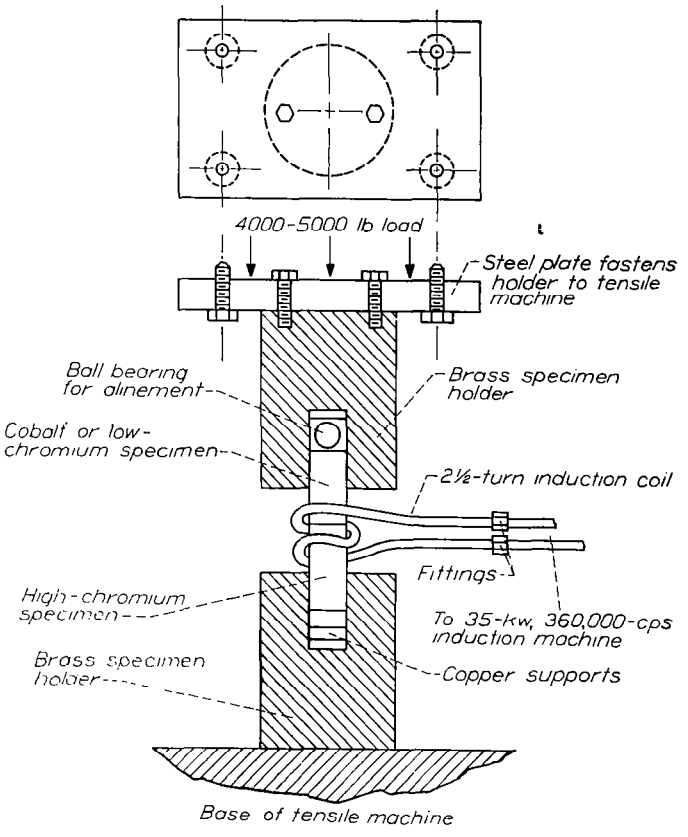

FIGURE 2.—Pressure-welding apparatus.

During the heat-up time, which varied from ½ to 1½ minutes, the tendency for the load to increase as thermal expansion of the cylinders took place was reduced by the tensile-machine operator, who kept the pressure reasonably constant (within ±200 pounds). Because a skin effect could be produced by raising the specimen temperature too rapidly, the power to the induction machine was turned on and off to allow an even heat distribution across the weld surface. When the temperature, which was read with an optical pyrometer, reached a point between 982° and 1038° C (1800° to 1900° F), the load was reduced to 4000 pounds to prevent excessive bulging. This load was maintained during the welding period of 1½ to 2½ minutes at 1121° to 1204° C (2050° to 2200° F). Bulging was kept at a minimum to prevent curving of the interface. Uneven heating or misalinement of specimens caused bent or distorted welds. Satisfactory welds were strong enough to be hammered and bent.

First welding attempts were unsuccessful because the surfaces were not lapped to a gage-block finish and, as a result, considerable oxides were formed in the welds. An attempt was also made to surround the apparatus shown in figure 2 with a vacuum-tight shell into which argon or helium could be bled during welding. However, in spite of insulating the container and the coil from the work, extensive arcing in these atmospheres prevented welding. This method was then abandoned in favor of the one used.

Metallographic examination after welding.—Flat planes were ground lengthwise on the welded specimens for metallographic examination (fig. 3). In the etched and unetched

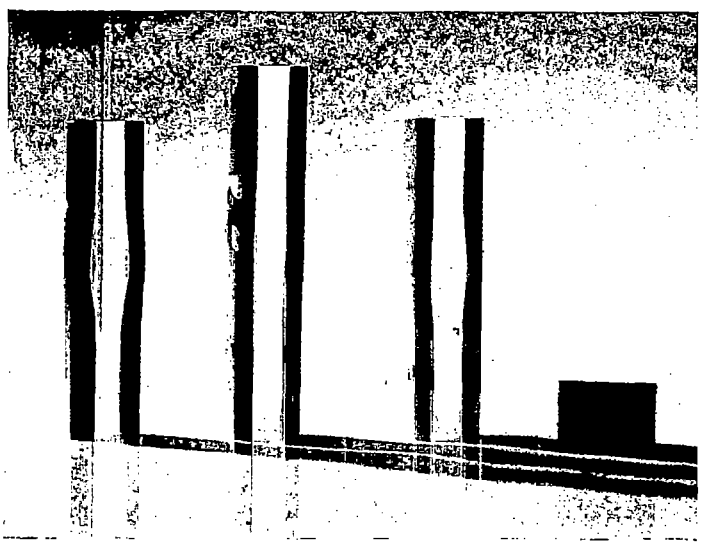

FIGURE 3.—Pressure-welded specimens with flat planes polished for metallographic examination.

conditions, the weld interfaces were examined for oxides, weld curvature, and other imperfections. Examples of satisfactory and unsatisfactory welds are shown in figure 4. Diffusion zones formed during welding were measured with a micrometer eyepiece and a research metallograph. The thickness of these zones, ranging from less than 0.0001 to 0.00046 inch (<0.00254 to 0.0117 mm), were considered negligible (fig. 4 (b)).

Machining prior to anneal.—Specimens 1¼ inches long and $^{11}/_{16}$ to $^{13}/_{16}$ inch in diameter, which included the weld interface, were turned from the welded specimens. Care was exercised during machining to make certain that the axes of these cylinders were perpendicular to the weld interfaces.

Calibration of instruments.—The thermocouple wires used during the diffusion anneal, subsequently to be described, were taken from a coil calibrated by the National Bureau of Standards. The potentiometer used to read the temperature was calibrated at the Lewis laboratory.

Diffusion anneal.—

1. Furnaces: Most of the specimens were annealed in a furnace using silicon carbide heating elements controlled by a self-balancing, self-standardizing, indicating pyrometer. The furnace, an eight-element unit, and the controller were wired so that four elements cycled on and off while the other four received power at all times. A zirconium silicate tube was placed in the furnace as shown in figure 5. The specimens to be annealed were placed in a porous-brick holder along with a platinum—platinum-rhodium thermocouple. A period of 1 to 3 hours was required to stabilize the furnace temperature after loading. Fluctuations of more than ±4° C (±7.2° F) were rare and were of short duration. Time-temperature plots were made for all of the specimens except those annealed at 1000° C for 87.7 days. A typical time-temperature plot for specimen 4 is shown in figure 6. The plots were integrated with a planimeter to find a weighted average temperature, which was then corrected for the thermocouple wire calibration and converted to °C (table I).

Specimens 8 and 9, which were annealed at 1000° C, were first annealed for a month in the silicon-carbide-element furnace and then transferred to a platinum-wound-resistance furnace. This furnace and a commercial light-beam-galvanometer-type photoelectric-cell controller were located in a room kept at constant temperature. Except for a temporary breakdown, the furnace was controlled within ±4° C (±7.2° F).

2. Atmospheres: During loading of the furnace, a large quantity of argon was blown through the tube to prevent oxidation of the specimen. The gas flow was decreased after the stopper was sealed in the loading end of the zirconium silicate tube. The argon flow was completely shut off, the rubber tube to the bubble jar was clamped shut, and the zirconium silicate tube and the argon line, including the drying towers, were evacuated by a pump capable of evacuating the system to a pressure of 1 millimeter of mercury when no leaks were present. This evacuation seated the rubber stopper and made it possible to locate any leaks in the thermocouple and the stopper seals. Argon was then bled into the evacuated zirconium silicate tube, which was then re-evacuated. This procedure was repeated five times to flush the tube. The vacuum pump was then closed and argon was allowed to pass through the system and out of the bubble jar.

Specimens 3 and 4 were placed in the furnace without the aid of the vacuum pump but upon removal after annealing were appreciably scaled (table I). After the system was evacuated, the drying towers (commercial metallic towers) were found to be leaking. Laboratory-type glass drying

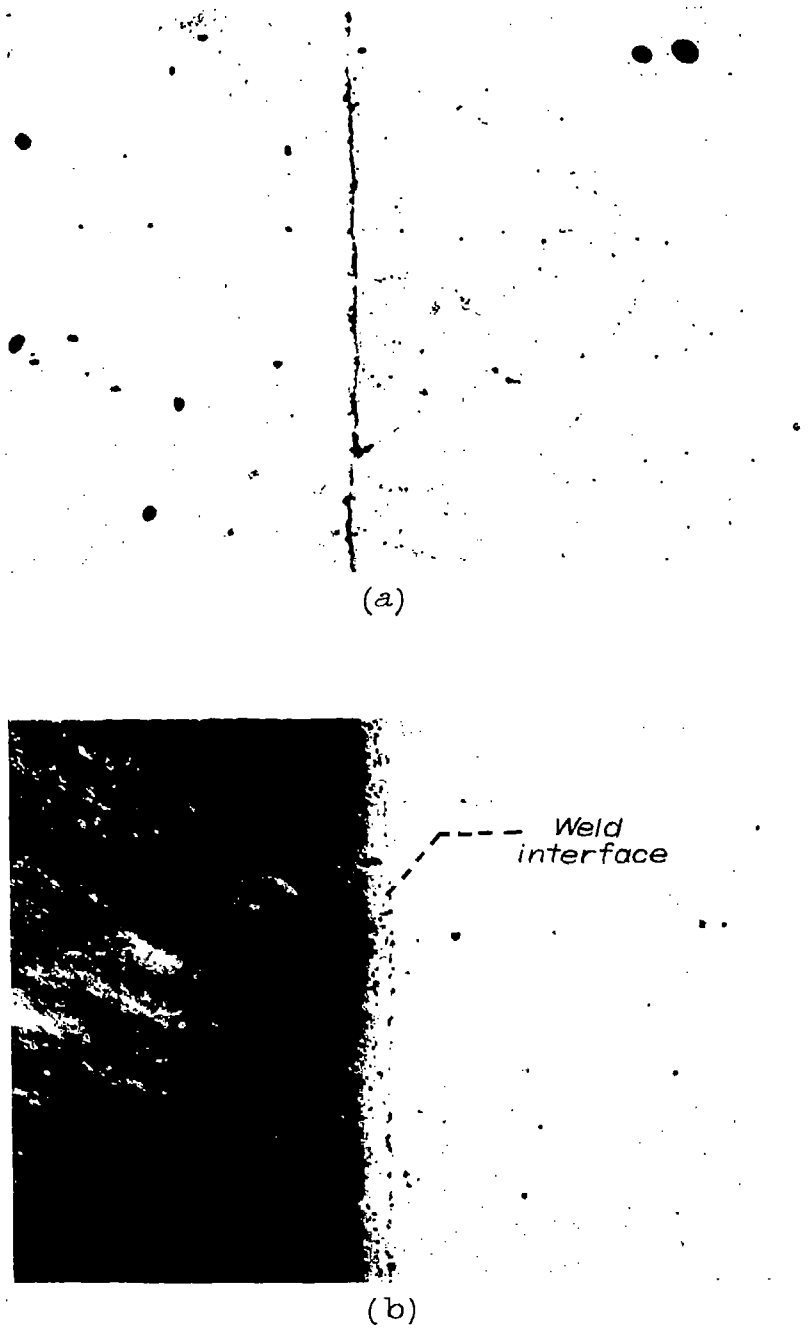

(a) Unsatisfactory weld interface. Etchant, none; magnification, ×750. Examination of unetched polished flat plane shows almost unbroken oxide layer in interface.
(b) Satisfactory weld interface. Etchant, 10-percent nitric acid in ethyl alcohol; magnification, ×750. Examination of heavily etched surface reveals approximately half of diffusion zone (distance between dark area and weld interface, approximately 0.00012 in. (0.0028 mm) wide) caused by welding. Etchant has attacked only cobalt half of weld.

FIGURE 4.—Appearance of satisfactory and unsatisfactory welds. (Magnification increased 10.4 percent in printing.)

towers were then installed and scaling was somewhat reduced. As an added precaution in annealing specimens 1, 2, 5, and 8 to 11, a mixture of hydrogen and helium, rather than argon, was passed through the zirconium silicate tube for a few hours after the system was sealed in order to scavenge oxygen from the bricks inside the tube. Argon was used after the hydrogen-helium purge and scaling was decreased to a negligible amount, especially when it is considered that loading and unloading the furnace could account for almost all the scale indicated for these specimens (table I).

Examination and reduction of diameter after anneal.—After the anneal, flat surfaces for metallographic examination were again ground on the specimens so that an estimate of the reduction in diameter needed to eliminate surface effects could be made. In most cases, $\frac{1}{32}$ to $\frac{3}{32}$ inch of metal was removed. Flat surfaces were again ground and examined (fig. 7), and where surface scaling was appreciable a thin turning was chemically analyzed for comparison with the original analyses. Oxide accumulations in the interface zone were also observed (fig. 8). The specimens were heavily etched and approximate measurements of total diffusion

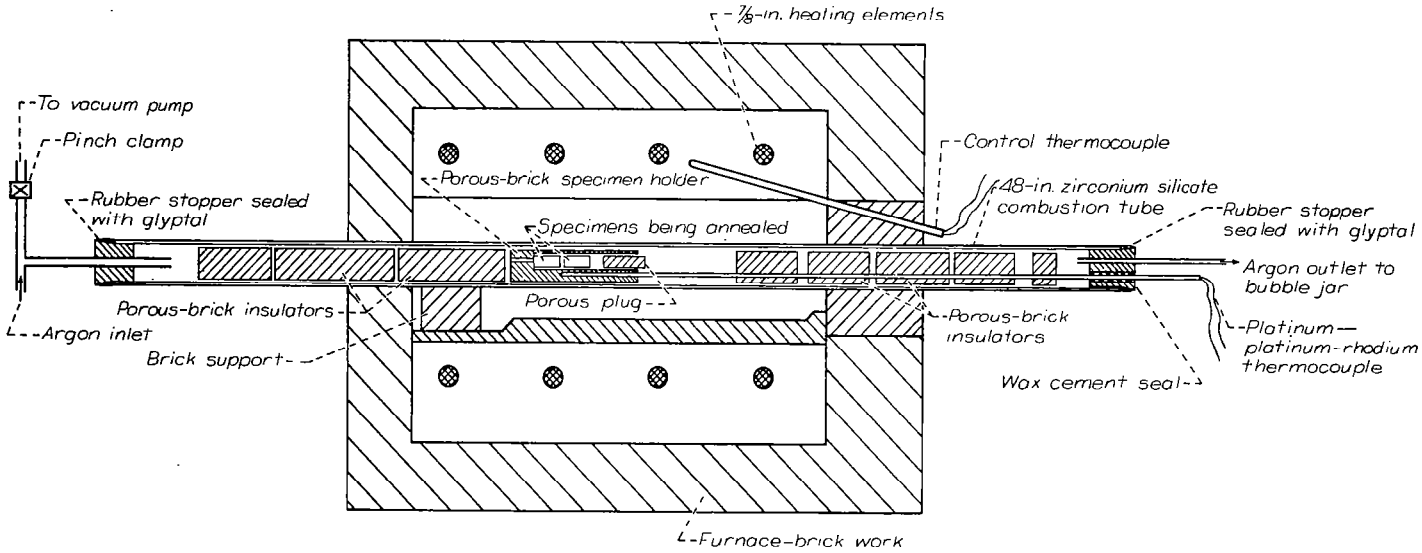

FIGURE 5.—Sectional view of annealing furnace showing specimen holder and thermocouple placement.

zones were made with a micrometer eyepiece. This measurement was made to determine the number of machining cuts required to cover the diffusion zone.

Machining successive layers through diffusion zone.— Before machining successive layers through the diffusion zone, excess metal was removed from the low-chromium half of the specimen to establish a reference surface from which cuts for analyses were made. From 0.1 to 0.125 inch (2.54 to 3.175 mm) of metal was left between the weld interface (determined metallographically) and the reference surface. Tungsten carbide cutting tools were used for all machining operations.

A series of turnings was made across the entire cross section starting at the reference surface perpendicular to the axis of the cylinder. After each turning, the distance machined was measured and the chips were gathered for chemical analysis. The cuts farthest from the interface were 0.010 inch thick (0.254 mm); cuts were reduced to a thickness from 0.003 to 0.005 inch (0.0762 to 0.127 mm) in the diffusion zone. In all the specimens except specimen 3, the entire zone was covered by the smallest cuts made.

Three methods of machining successive cuts through the diffusion zone were used. In the first method, used for specimens 2 to 7, the cylinders with machined reference surfaces were chucked in a large rigid lathe. The head of this lathe contained a large cast-iron face plate that was machined for use as a surface plate. All cuts less than 0.007 inch thick were measured from the surface plate with a surface dial gage that could be read to 0.0001 inch and estimated to 0.00001 inch. Thus, removing the work from the chuck after each cut was unnecessary. A calibration of the dial showed that cuts of 0.003 inch needed no corrections and that cuts of 0.005 inch were in error by as little as 0.00006 inch, or approximately 1 percent. If human errors are taken into consideration, the maximum machining errors were believed to be no more than 2 percent. These

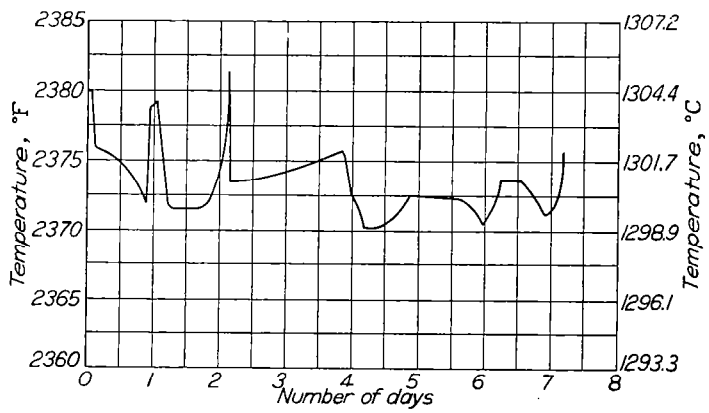

FIGURE 6.—Typical time-temperature plot for diffusion-anneal period in annealing furnace (specimen 4). Temperatures have not been corrected with platinum—platinum-rhodium wire calibration.

dial corrections were considered negligible and have been omitted in the calculations.

The second method, similar to the preceding one, was used for specimens 1, 8, and 9. The chips were machine off with a high-precision vertical jig borer (SIP Hydrostatic–7), which was kept in an air-conditioned room, and a calibrated surface gage was used to measure the cuts. Machining errors were measured with a micrometer and were determined by comparing the total amount of metal removed after making all the necessary cuts with the sum of all the small cuts measured with the surface dial gage. In specimen 8, with a total of 48 cuts, the error was 0.25 percent, whereas in specimen 9, the error was 2 percent in the same number of cuts.

The third method, used for specimens 10 and 11, was the most accurate as well as the most complicated. The vertical jig borer was again used, but the thickness of each cut was measured by an electronic height gage that measured the differences in height between stacks of gage blocks and the specimen surface to 0.00001 inch. As a further assurance that no discrepancies would occur, a height gage (surface

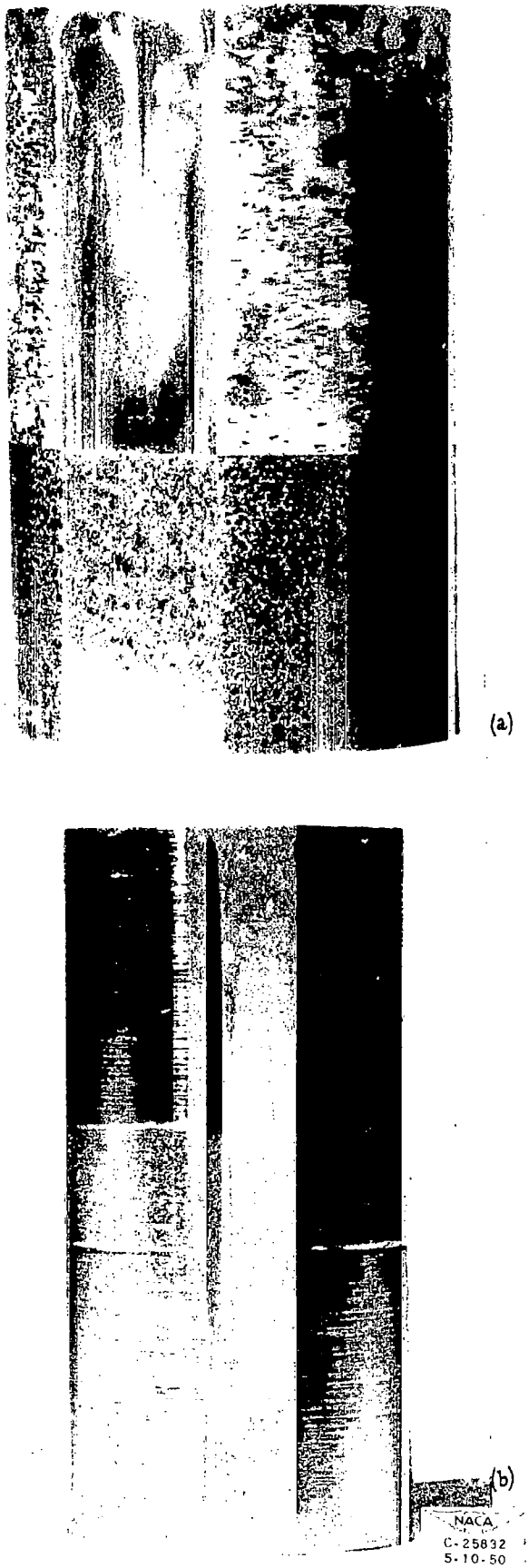

(a) Scale present after an anneal of several days. Scaling occurred chiefly during loading and unloading of annealing furnace.

(b) Specimen machined to smaller diameter than specimen in figure 7 (a). Another flat has been ground for metallographic examination and turnings have been taken from lower portion for chemical analysis.

FIGURE 7.—Specimen after diffusion anneal.

plate checker) was also used in conjunction with the electronic gage. With this gage, it was possible to measure the over-all height of the specimen to 0.00001 inch after each layer was machined off. Differences in over-all height were compared with the thickness of each cut as measured with the electronic height gage and the stacks of gage blocks. In the two specimens so machined, the error was 0 percent in 36 cuts for specimen 11 and 0.025 percent in 32 cuts for specimen 10.

Chemical analyses.—At least two and usually three analyses by a persulfate-oxidation method were made at the Lewis laboratory for every sample machined from the diffusion zone.

Methods of calculating diffusion coefficients.—The diffusion coefficients for all specimens were calculated by the Grube method (reference 3). In addition, calculations using the Matano method (reference 3) were made for specimens 3 and 5. The Matano method was not used throughout because it was extremely time consuming and the results closely paralleled those calculated by the Grube method.

The metric system was used in plotting concentration-penetration curves and diffusion coefficients were calculated in this system to conform with previous work. The data points were plotted at distances halfway between successive cuts, which were measured from a reference plane. Leveling-off points of the curves were drawn from mathematical averages of several data points, some of which are not shown in the figures.

Diffusion coefficients were calculated from the concentration-penetration curves using the following equation (Grube method):

$$\frac{C-C_0}{C_1-C_0}=\frac{1}{2}\left(1\pm\frac{2}{\sqrt{\pi}}\int_0^{\omega}e^{-\omega^2}d\omega\right)$$

where

C chromium concentration, atomic percent

C_0 chromium concentration of low-chromium bar, atomic percent

C_1 chromium concentration of high-chromium bar, atomic percent

$\omega = \dfrac{x}{2\sqrt{Dt}}$

D diffusion coefficient, (cm^2/sec)

x distance from Grube interface, (cm)

t time, (sec)

Positive values were used for calculations made from the high-chromium portions of the concentration-penetration curves to the right of the Grube interface, whereas negative values were used for calculations made from the low-chromium portions of the curves to the left of the Grube interface.

The Grube interface is the distance in the diffusion zone at which the concentration is halfway between the lower and upper concentrations C_0 and C_1, respectively (figs. 9 (d) and 9 (f)).

Let

$$H\left(\frac{x}{2\sqrt{Dt}}\right)=\pm\frac{2}{\sqrt{\pi}}\int_0^{\omega}e^{-\omega^2}d\omega$$

$$\omega=\frac{x}{2\sqrt{Dt}}$$

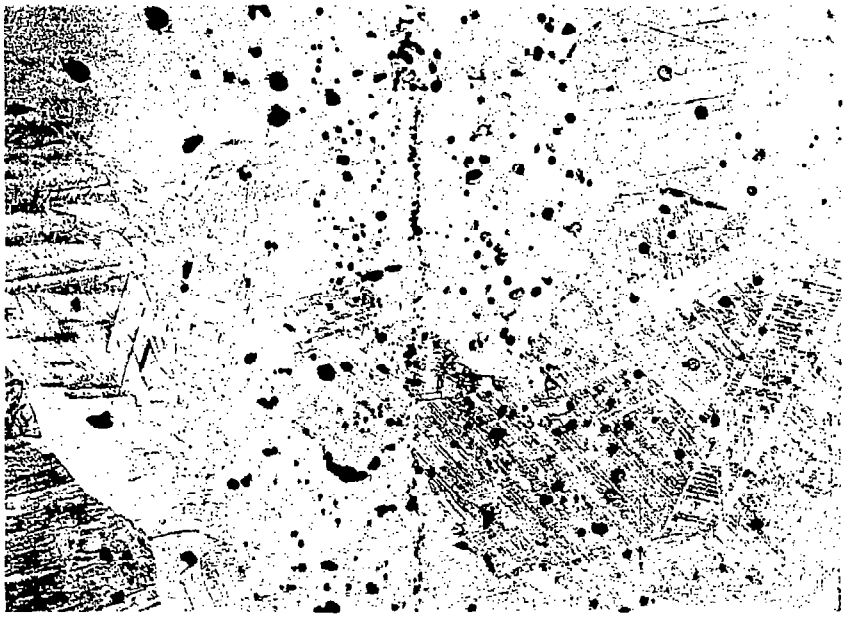

FIGURE 8.—Central portion of diffusion zone of specimen 10. Annealed 7.17 days at 1297° C; etchant, 5-percent nitric acid in ethyl alcohol followed by aqua regia in glycerine; magnification, ×100. Photograph shows accumulation of oxides near center of diffusion zone. (Magnification increased 6.2 percent in printing.)

Then

$$\frac{C-C_0}{C_1-C_0}=\frac{1}{2}\left[1\pm H(\omega)\right]$$

$$H(\omega)=\pm 2\left(\frac{C-C_0}{C_1-C_0}-0.5\right)$$

The value of ω may be obtained from probability tables and inasmuch as

$$\omega=\frac{x}{2\sqrt{Dt}}$$

then

$$D=\frac{x^2}{\omega^2}\frac{1}{4t}$$

The final equation indicates that D is very sensitive to x, the machined distance.

RESULTS

Concentration-penetration curves of all specimens are plotted in figure 9. Several of these curves, such as those for specimens 3, 4, 7, 8, and 10 (figs. 9 (d), 9 (e), 9 (i), 9 (j), and 9 (g), respectively) are very symmetrical. When data from these curves are plotted on a probability graph in the form

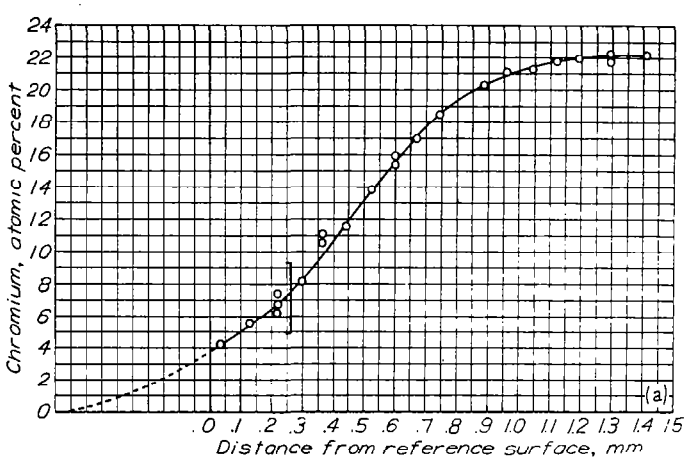

(a) Specimen 1; annealed at 1360° C for 3.384×10⁵ seconds (3.92 days). Data to left of bracket are inaccurate because of quench crack that formed after diffusion took place.

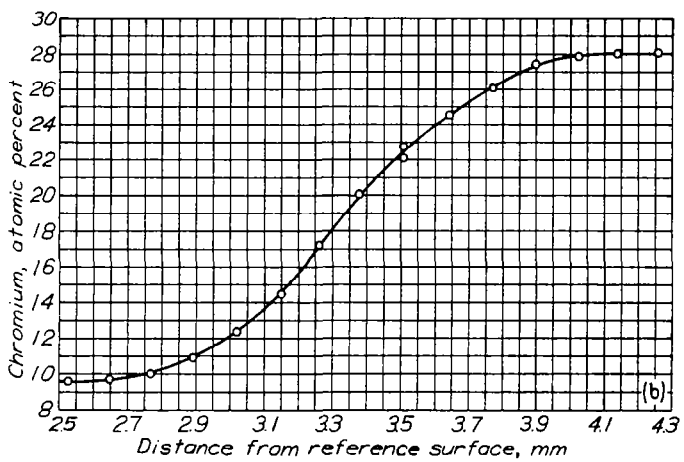

(b) Specimen 2; annealed at 1360° C for 3.384×10⁵ seconds (3.92 days).

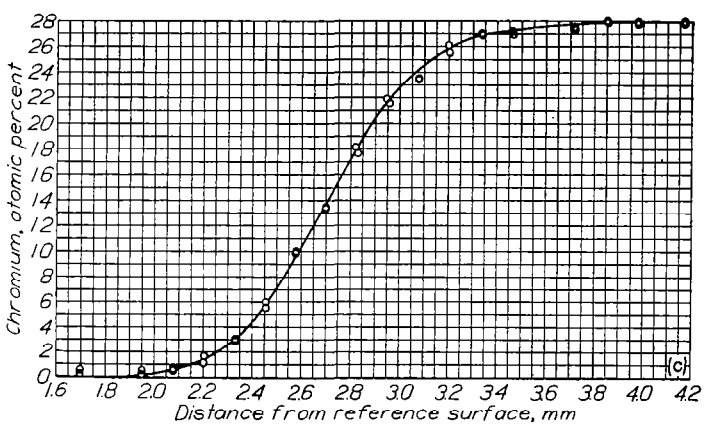

(c) Specimen 11; annealed at 1369° C for 3.321×10⁵ seconds (3.84 days).

FIGURE 9.—Concentration-penetration curves.

FIGURE 9.—Continued. Concentration-penetration curves.

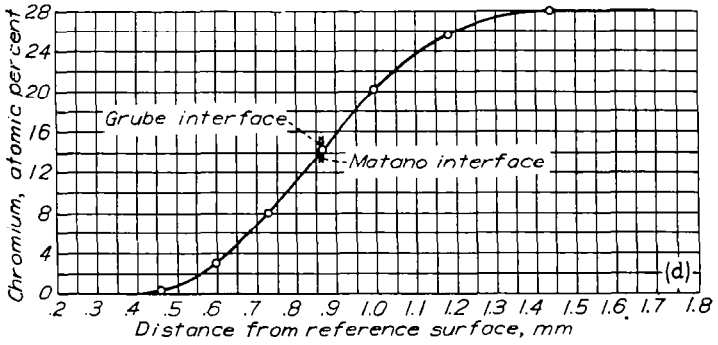

(d) Specimen 3; annealed at 1303° C for 3.522×10^5 seconds (4.08 days).

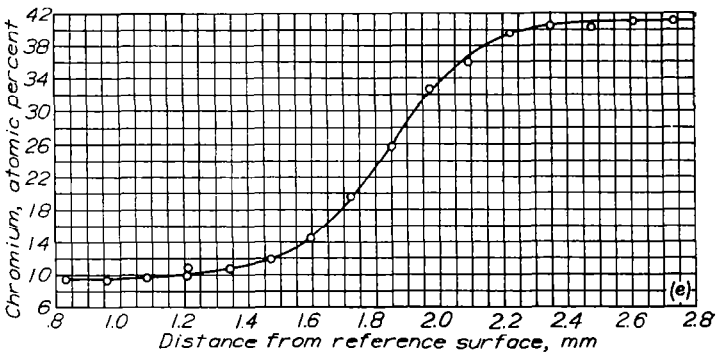

(e) Specimen 4; annealed at 1298° C for 6.216×10^5 seconds (7.19 days).

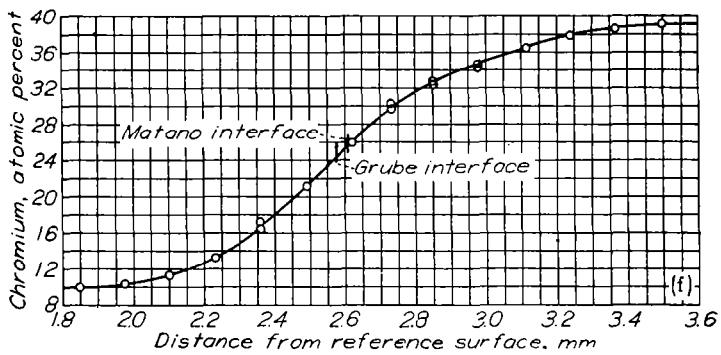

(f) Specimen 5; annealed at 1299° C for 9.549×10^5 seconds (11.05 days).

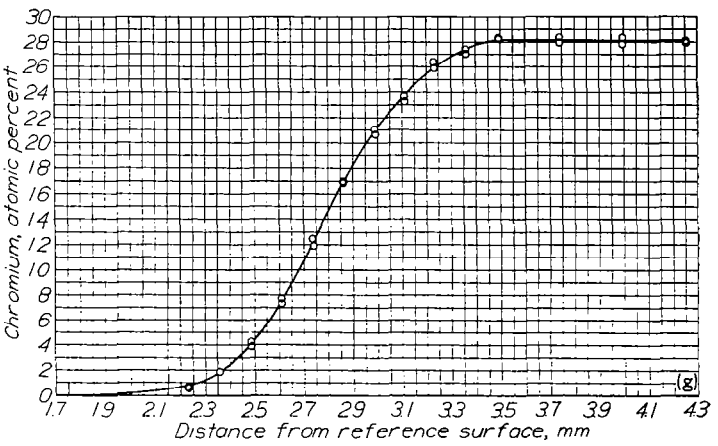

(g) Specimen 10; annealed at 1297° C for 6.198×10^5 seconds (7.17 days).

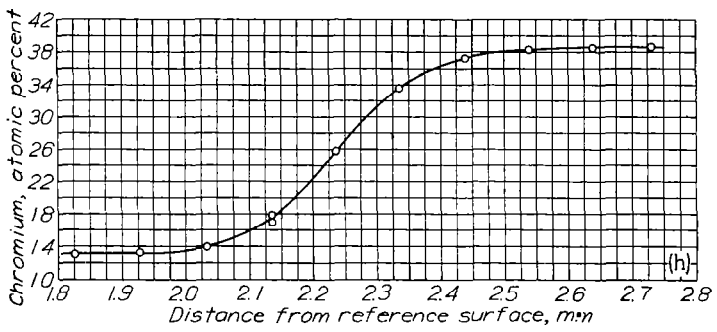

(h) Specimen 6; annealed at 1150° C for 1.0446×10^6 seconds (12.09 days).

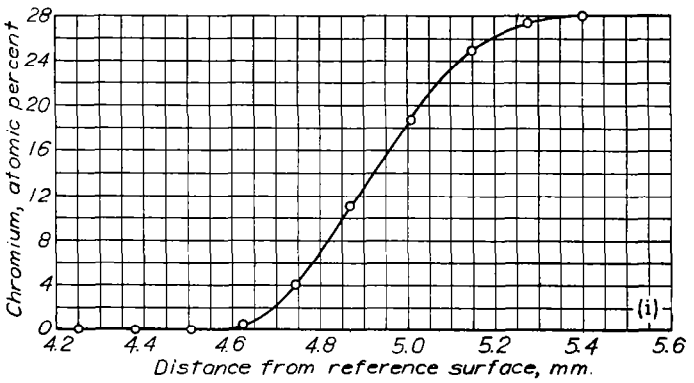

(i) Specimen 7; annealed at 1151° C for 2.152×10^6 seconds (24.91 days).

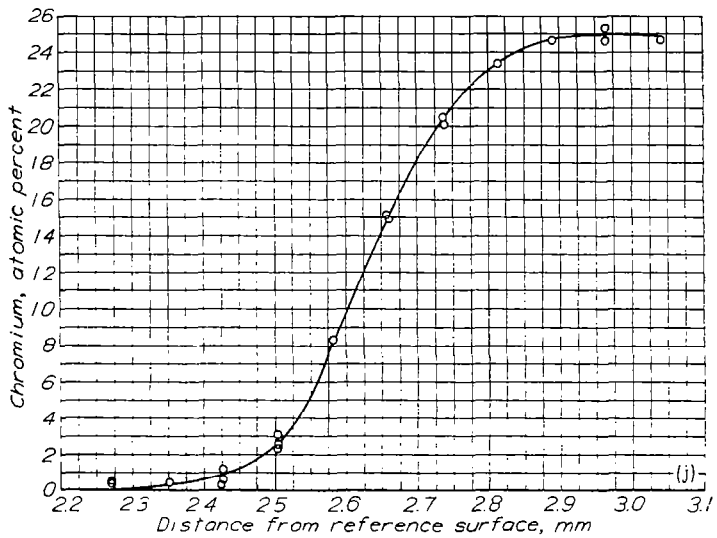

(j) Specimen 8; annealed at 1000° C for 7.664×10^6 seconds (87.70 days).

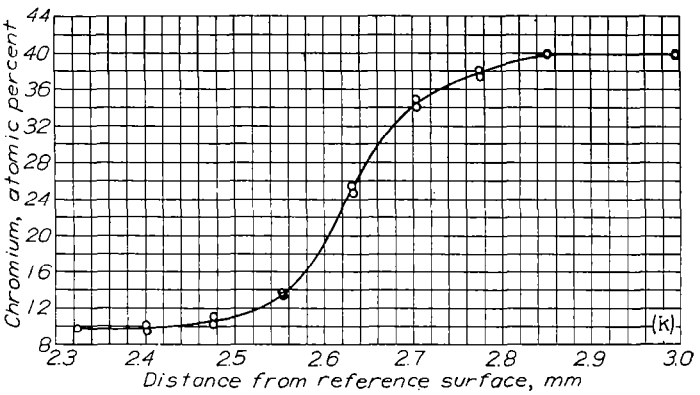

(k) Specimen 9; annealed at 1000° C for 7.664×10^6 seconds (87.70 days).

FIGURE 9.—Concluded. Concentration-penetration curves.

$(C-C_0)/(C_1-C_0)$ against the distance from the Grube interface, approximately straight lines are obtained (fig. 10). In these cases, the diffusion coefficient D is almost invariant with the concentration C. The curves pass through the point $\left(x=0, \frac{C-C_0}{C_1-C_0}\times 100=50\right)$.

Other curves, such as that for specimen 5 (fig. 9 (f)), bend slightly from a smooth curve in the upper right, or high-chromium portions, of the diffusion curves. These bends also show up in the probability plots (fig. 10 (f)). Deviations from smooth concentration-penetration curves and from straight lines in the probability plots could be a function of concentration. The deviations, however, are believed to be caused by oxide segregations that may have been present in the high-chromium half of the welded specimens before the diffusion anneal or that may have formed during the annealing by migrations of oxides that were originally randomly scattered throughout the matrix of the metal. The metallographic examinations and the smooth lower portions of most of the curves indicate that migration is the most probable case.

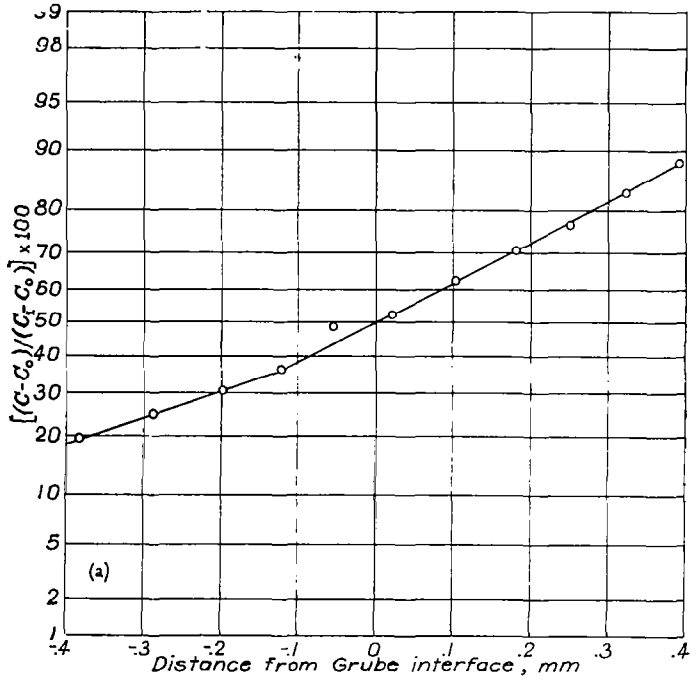

(a) Specimen 1; annealed at 1360° C for 3.92 days.

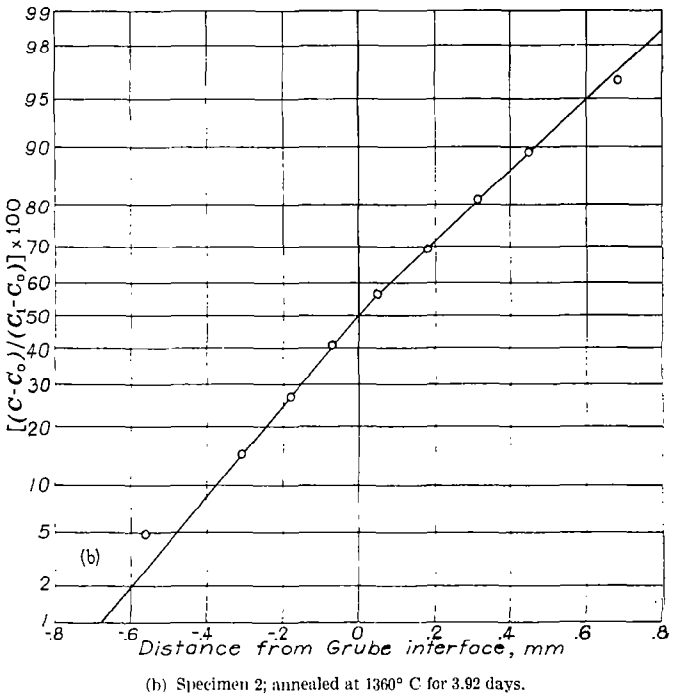

(b) Specimen 2; annealed at 1360° C for 3.92 days.

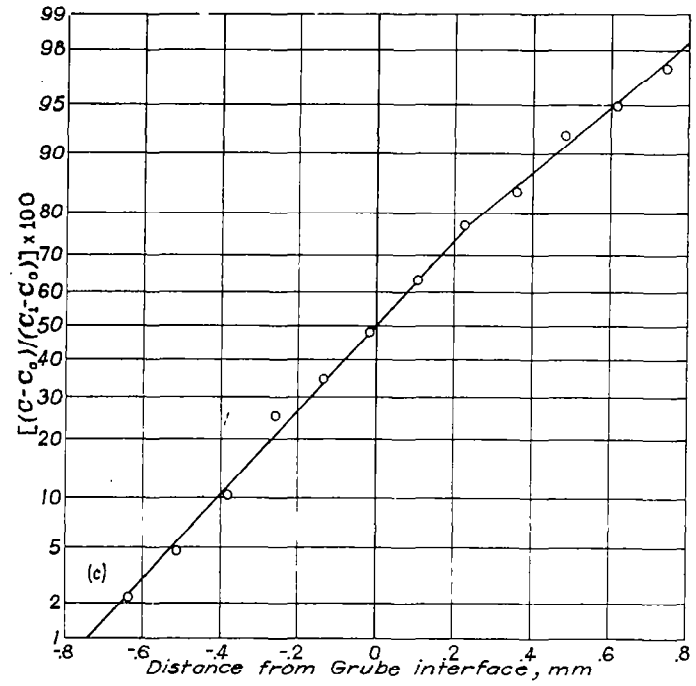

(c) Specimen 11; annealed at 1369° C for 3.84 days.

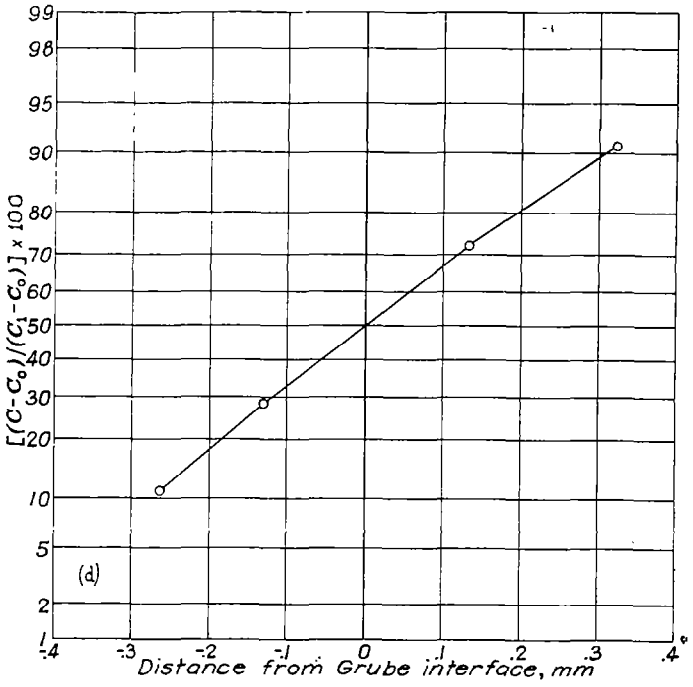

(d) Specimen 3; annealed at 1303° C for 4.08 days.

FIGURE 10.—Plots of $(C-C_0)/(C_1-C_0)$ against distance from Grube interface.

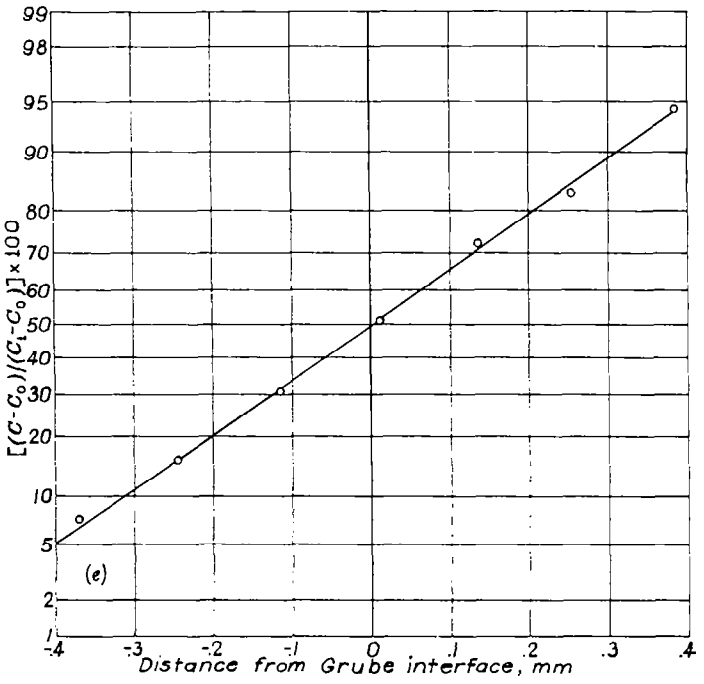

(e) Specimen 4; annealed at 1298° C for 7.19 days.

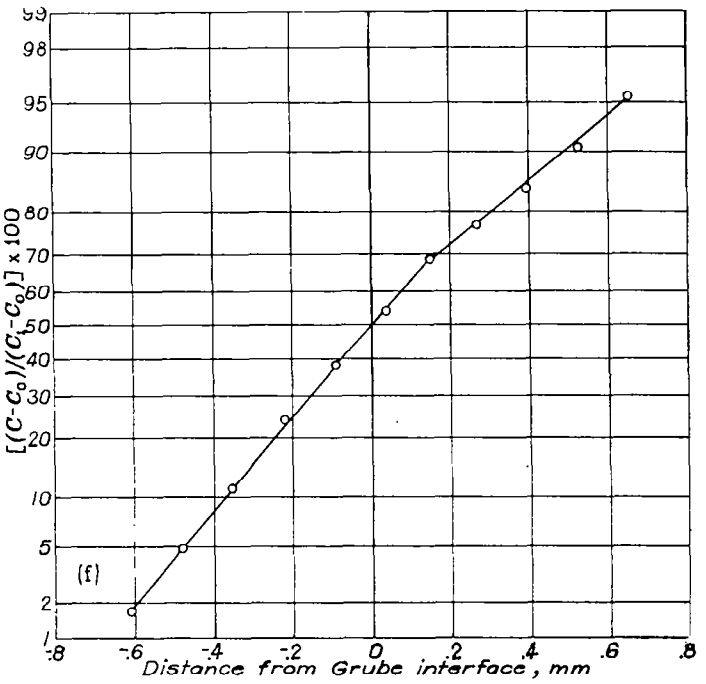

(f) Specimen 5; annealed at 1299° C for 11.05 days.

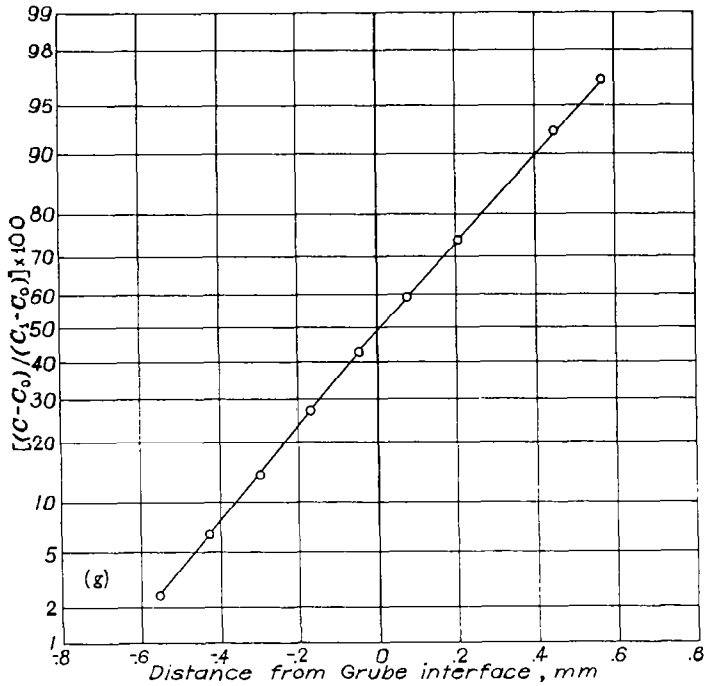

(g) Specimen 10; annealed at 1297° C for 7.17 days.

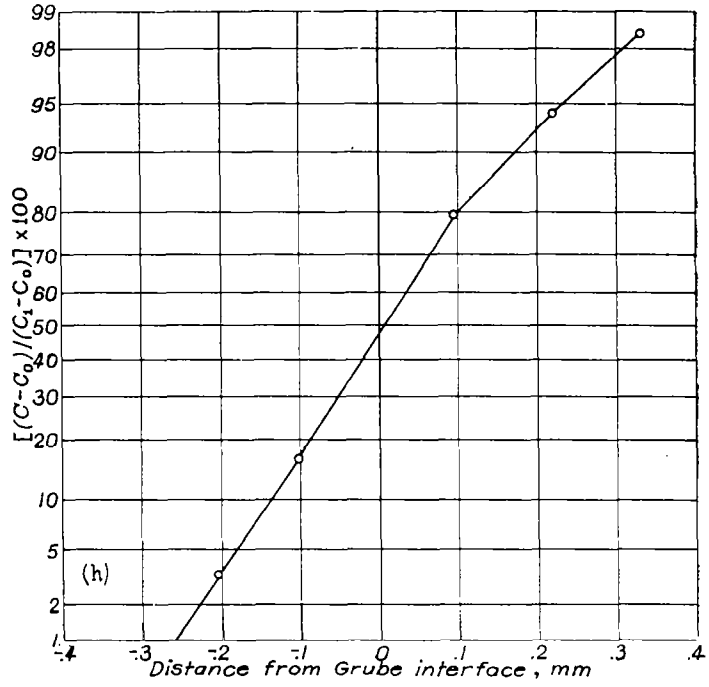

(h) Specimen 6; annealed at 1150° C for 12.09 days.

FIGURE 10.—Continued. Plots of $(C-C_0)/(C_1-C_0)$ against distance from Grube interface.

Diffusion coefficients calculated by the Grube method from the concentration-penetration curves are plotted against concentration in figure 11. Values of diffusion coefficients obtained from the extreme ends of the diffusion-penetration curves and from portions near the Grube interfaces were omitted from the plot because they are inherently inaccurate. The degree of reproducibility of data appears good, as shown in the cases of specimens 3 and 10, and 4 and 5, which were annealed at 1300° ± 3° C.

Specimens 1 and 2, prior to annealing at 1360° C, were annealed at 900° C for several weeks. Meanwhile, diffusion coefficients were obtained at 1300° and 1150° C and rough calculations from these preliminary data showed that an annealing time of about 8 years at 900° C would be required to produce a diffusion zone comparable in thickness to the smallest zone obtained at the higher temperatures. Inasmuch as the annealing time at 900° C was insignificantly small, the specimens were reannealed at 1360° C to obtain additional data. Because the specimens were originally intended for heat treatment at 900° C, the composition range covered by specimens 1 and 2 is small compared with what would be possible at 1360° C.

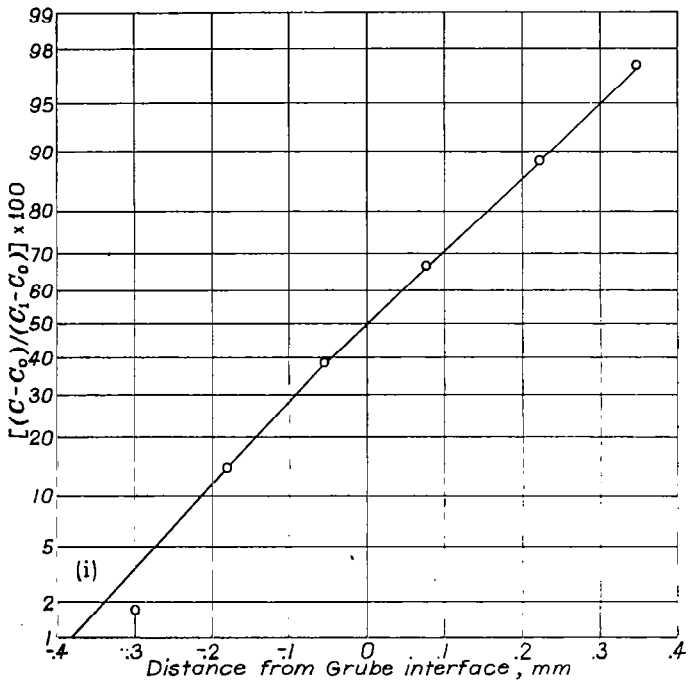

(i) Specimen 7; annealed at 1151° C for 24.91 days.

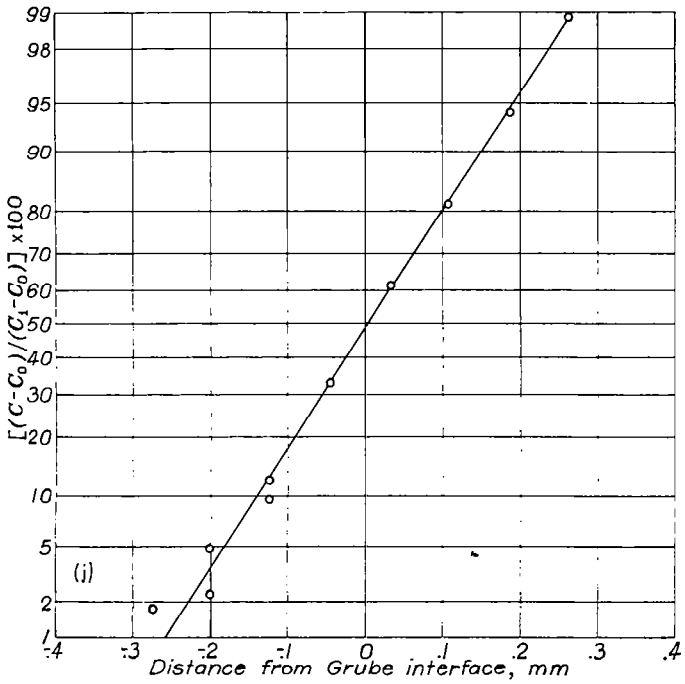

(j) Specimen 8; annealed at 1000° C for 87.7 days.

FIGURE 10.—Continued. Plots of $(C-C_0)/(C_1-C_0)$ against distance from Grube interface.

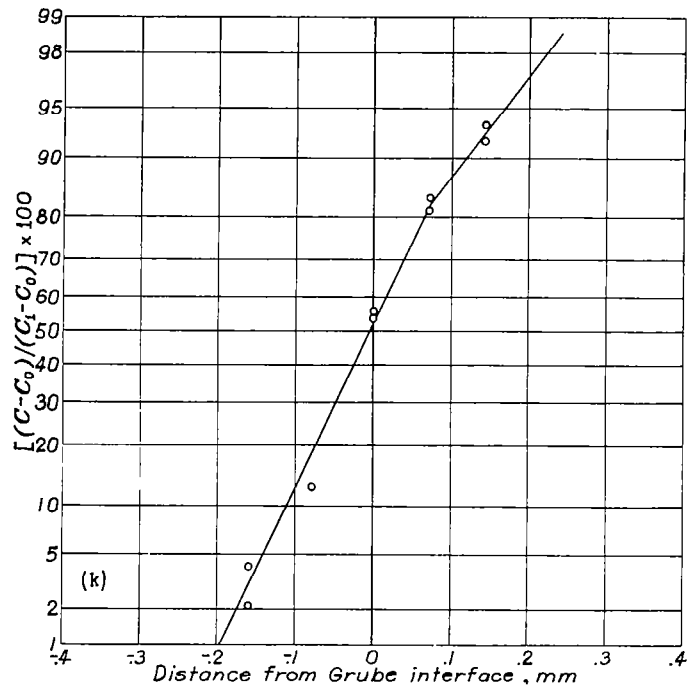

(k) Specimen 9; annealed at 1000° C for 87.7 days.

FIGURE 10.—Concluded. Plots of $(C-C_0)/(C_1-C_0)$ against distance from Grube interface.

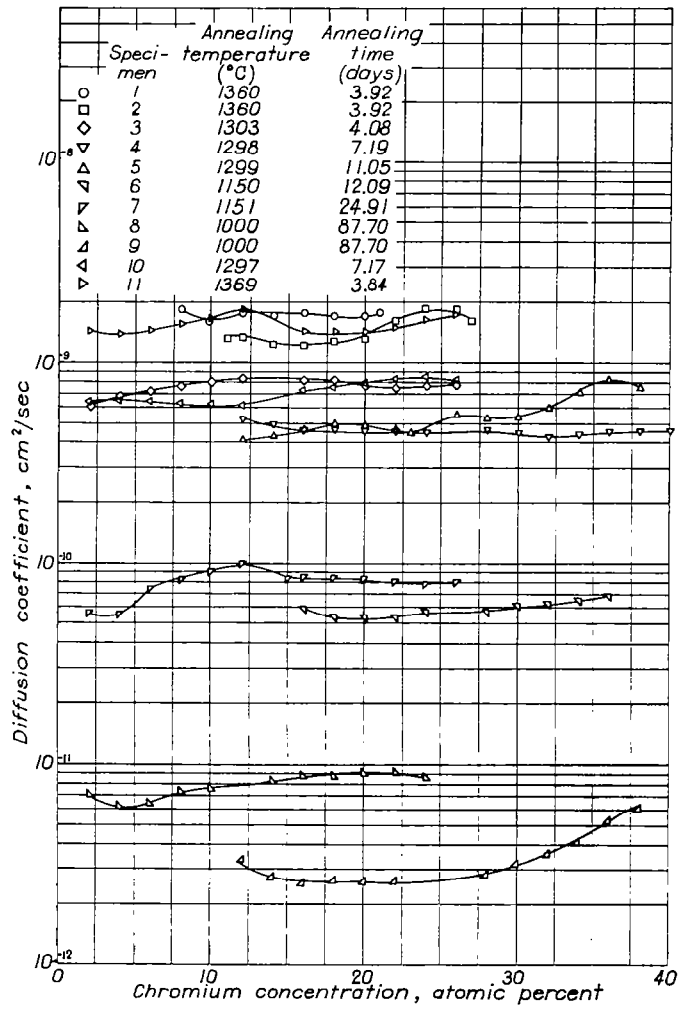

FIGURE 11.—Diffusion coefficients against concentration. (Data to left of 8 atomic percent not plotted for specimen 1 because of quench crack that formed after diffusion took place.)

The upper half of the curve of specimen 1 (fig. 9 (a)) is satisfactory and calculations were made from it by the Grube method. The lower portion, however, was inaccurate as a result of a quench crack formed by cooling the specimen in an air blast as it was removed from the annealing furnace.

The composition of specimen 9 extends into the $\alpha+\gamma$ field (fig. 1), but because it is close to the α-phase boundary, only a small percentage of γ would be present. Since the γ-phase was not observed during the metallographic examinations, the calculated diffusion coefficients would therefore be reasonably accurate.

In spite of several metallographic inspections, a strip of oxide $\frac{1}{32}$ inch deep extending halfway about the periphery of specimen 11 was noticed as it was being machined. Approximately 5.4 percent of the area of the interface was blocked. Inasmuch as this area is a small portion of the total area, the data for specimen 11 were not discarded.

A plot of diffusion coefficients against concentration (fig. 12) shows the small differences between values determined by the Grube and the Matano methods.

The relation between diffusion coefficients and reciprocal temperatures are shown in figure 13. The upper and lower curves are plotted from data obtained for 16-atomic-percent chromium because these values are close to averages of the flat portions of the curves of figure 11. The upper curve represents diffusion coefficients obtained from specimens of cobalt welded to cobalt-chromium alloys, whereas the lower curve represents alloys approximately 9- to 14-atomic-percent chromium welded to alloys of approximately 28- to 41-atomic-percent chromium.

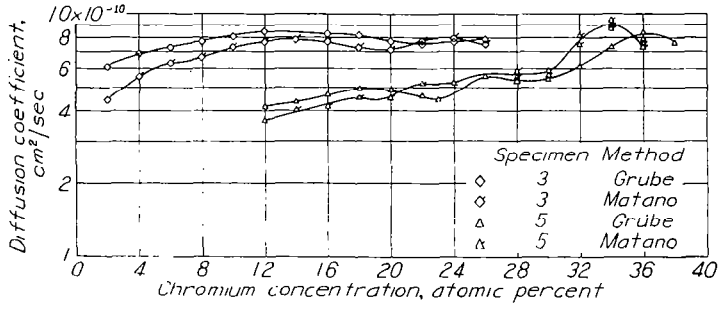

FIGURE 12.—Comparison of diffusion coefficients calculated by the Grube and Matano methods.

By use of the dashed curve, which was drawn halfway between the upper and lower solid curves in figure 13, and of the exponential equation (reference 1)

$$D=Ae^{-\frac{Q}{RT}}$$

the activation heat of diffusion Q and the constant A were determined to be

$$Q=63{,}600 \text{ (cal/mole)}$$
$$A=0.443 \text{ (cm}^2\text{/sec)}$$

The value of Q was determined from the slope of the dashed curve because

$$2.303\frac{(\log D_1-\log D_2)}{\frac{1}{T_1}-\frac{1}{T_2}}=-\frac{Q}{R}$$

and A was determined from the preceding exponential equation, using the value of Q obtained and values of D and $1/T$ chosen from the dashed curve.

The diffusion behavior of chromium in α cobalt-chromium alloys may be compared with that of other metal systems in figure 14, where values from the dashed curve of figure 13 are replotted for the comparison. The curves for the other alloy systems were taken from the graphs of references 3 to 9.

DISCUSSION OF RESULTS

Diffusion coefficients are relatively constant within the concentration ranges of each specimen. Appreciable differences between diffusion coefficients, however, were obtained from specimens of pure cobalt welded to α cobalt-chromium alloys and specimens of low-chromium α-alloys welded to high-chromium α-alloys at each nominal annealing temperature; the diffusion coefficients for specimens of pure cobalt welded to α cobalt-chromium alloys were larger (figs. 11 and 13).

The differences in diffusion coefficients are not the results of such experimental variables as:

(1) Differences in sources of materials because single supplies of cobalt and chromium were used in this study

(2) Differences in annealing temperatures because specimens 1 and 2 and specimens 8 and 9 were annealed together at identical temperatures and the remaining specimens were annealed at temperatures very close to the desired nominal temperatures

(3) Differences due to the closeness of the high-chromium specimens to the α-γ region because specimens 1 and 2 were well within the α region

A somewhat similar observation may be made from figure 14, where curves 4 and 5 represent the diffusion of pure copper into pure gold, and copper from a gold-copper alloy into gold, respectively.

The experimental data give additional confirmation to the Dushman-Langmuir equation

$$D=\frac{Q}{Nh}\delta^2 e^{-\frac{Q}{RT}}$$

where

D	diffusion coefficient, (cm²/sec)
Q	activation heat of diffusion, (cal/mole)
N	Avogadro's number
h	Planck's constant, (cal-sec)
δ	distance of closest approach of atoms, $\frac{a_o}{\sqrt{2}}$, (cm)
a_o	lattice parameter
R	gas constant, (cal/(mole)(°K))
T	temperature, (°K)

The following value of Q has been calculated by arbitrarily selecting a point on the dashed curve of figure 13 to obtain a D value for a given temperature:

$$Q=63{,}400 \text{ (cal/mole)}$$

Values used in the calculation are as follows:

$$D=6\times10^{-11}\ (\text{cm}^2/\text{sec})$$

$$\frac{1}{^\circ K}=7.1\times10^{-4}$$

$$a_o=3.54\times10^{-8}\ (\text{cm})\ \text{(reference 10)}$$

The value of Q compares favorably with the value of $Q=$ 63,600 (cal/mole) obtained from the slope of the dashed curve.

The diffusion rates of chromium in α cobalt-chromium were very low compared with those of most alloy systems for which diffusion data had been previously obtained. For example, it can be determined from figure 14 that a high temperature (1031° C) is required to produce log $D=-11$ for chromium in cobalt, whereas annealing temperatures of 362°, 628°, and 784° C are required for Mg in Al, Zn in Cu, and Pt in Au, respectively. The sluggishness of diffusion is congruous with the fact that cobalt-chromium base alloys have good high-temperature characteristics.

The activation heat of diffusion for chromium in α cobalt-chromium alloys is greater than that for most systems previously investigated, with tungsten alloys being the chief exceptions (reference 11). Higher activation heats of diffusion show up in the form of steeper slopes on the curve of log D against 1/°K (fig. 14).

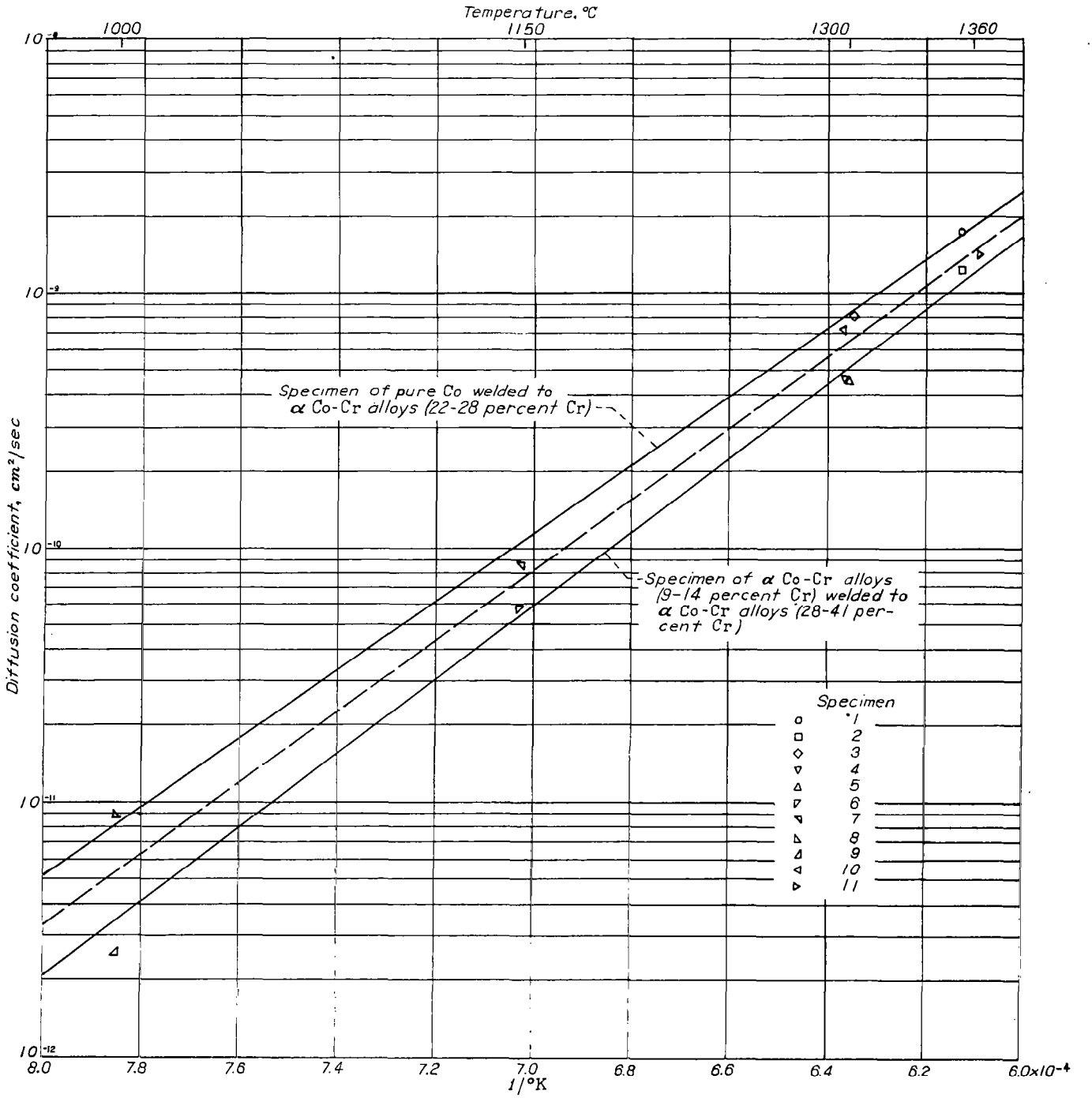

FIGURE 13.—Diffusion coefficients against 1/°K. Diffusion coefficients were plotted from data for 16-atomic-percent chromium.

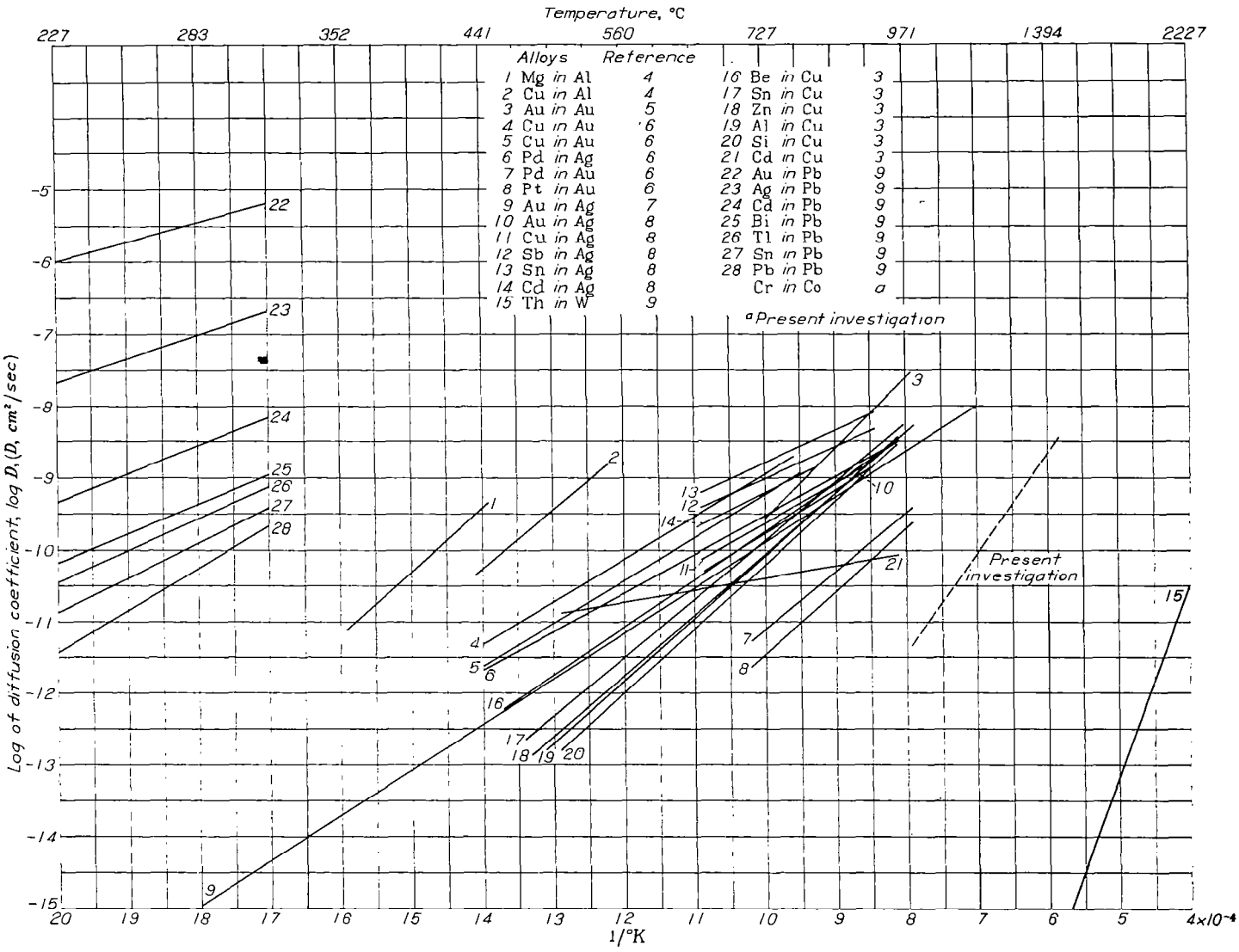

FIGURE 14.—Comparison of diffusion behavior of chromium in α cobalt-chromium alloys with other substitutional solid-solution alloys.

SUMMARY OF RESULTS

Diffusion of chromium in α cobalt-chromium solid solutions was investigated at temperatures of 1360°, 1300°, 1150°, and 1000° C and the following results obtained:

1. The exponential equation relating diffusion coefficient D and temperature T is as follows:

$$D=0.443e^{-\frac{63,600}{RT}}$$

where R is the gas constant. The activation heat of diffusion is 63,600 calories per mole.

2. When compared with the diffusion data previously obtained by other investigators for most alloy systems, the diffusion rates of chromium in α cobalt-chromium were found to be low; considerably higher temperatures were required to produce diffusion coefficients of the same order of magnitude as were previously found for most substitutional alloys.

3. Diffusion coefficients are relatively constant within the concentration ranges covered by each specimen.

4. Chromium diffusivity from α cobalt-chromium alloys into pure cobalt is greater than chromium diffusivity from high-chromium α-alloys to low-chromium α-alloys for all concentration gradients studied.

5. The results of this investigation are further confirmation of the Dushman-Langmuir equation. The value for the activation heat of diffusion calculated from this equation agrees closely with the experimentally determined value (63,400 cal/mole as calculated against 63,600 cal/mole obtained from experimentation).

LEWIS FLIGHT PROPULSION LABORATORY
NATIONAL ADVISORY COMMITTEE FOR AERONAUTICS
CLEVELAND, OHIO, *June 23, 1950*

REFERENCES

1. Wells, Cyril, and Mehl, Robert F.: Rate of Diffusion of Carbon in Austentite, in Plain Carbon, in Nickel and in Manganese Steels. Trans. A. I. M. E., Iron and Steel Div., vol. 140, 1940, pp. 279–306.
2. Elsea, A. R., Westerman, A. B., and Manning, G. K.: The Cobalt-Chromium Binary System. Metals Tech., vol. 15, no. 4, June 1948, pp. 1–24.
3. Rhines, Frederick N., and Mehl, Robert F.: Rates of Diffusion in the Alpha Solid Solutions of Copper. Trans. A. I. M. E., Inst. Metals Div., vol. 128, 1938, pp. 185–221; discussion, pp. 221–222.
4. Brick, R. M., and Phillips, Arthur: Diffusion of Copper and Magnesium into Aluminum. Trans. A. I. M. E., Inst. Metals Div., vol. 124, 1937, pp. 331–347; discussion, pp. 347–350.
5. McKay, H. A. C.: The Self-Diffusion Coefficient of Gold. Trans. Faraday Soc (London), vol. XXXIV, 1938, pp. 845–849.
6. Jost, W.: Die Diffusionsgeschwindigkeit einiger Metalle in Gold und Silber. Zeitschr. Phys. Chem., Bd. 21, Heft 1 und 2, Abt. B, April 1933, S. 158–160.
7. Jost, W.: Über den Platzwechselmechanismus in festen Körpern. Die Diffusion von Gold und Silber. Zeitschr. Phys. Chem., Bd. 9, Heft 1, Abt. B, Juli 1930, S. 73–82.
8. Jost, W.: Diffusion und Chemische Reaktion in festen Stoffen. Theodor Steinkopff (Dresden und Leipzig), 1937, S. 115. (Reproduced by Edwards Bros. (Ann Arbor, Mich.), 1943.)
9. Mehl, Robert F.: Diffusion in Solid Metals. Trans. A. I. M. E., Inst. Metals Div., vol. 122, 1936, pp. 11–56.
10. Anon.: Metals Handbook, 1948 Edition. Am. Soc. Metals (Cleveland), 1948, p. 1191.
11. Barrer, Richard M.: Diffusion in and through Solids. Cambridge Univ. Press (London), 1941, p. 275.

TABLE I—ANNEALING DATA

Specimen	Weighted average annealing temperature (° C)	Annealing time (days)	Annealing time (sec)	Approximate thickness of scale formed during annealing (in.)
1	1360.4	3.917	3.384×10^5	0.002
2	1360.4	3.917	3.384×10^5	.002
3	1302.9	4.08	3.522×10^5	1/16
4	1297.8	7.194	6.216×10^5	1/32
5	1299.2	11.05	9.549×10^5	<.001
6	1149.7	12.09	1.0446×10^6	.010
7	1150.5	24.907	2.152×10^6	1/64
8	1000.3	87.704	7.664×10^6	.001–.002
9	1000.3	87.704	7.664×10^6	.001–.002
10	1296.9	7.174	6.198×10^5	.002
11	1368.9	3.844	3.321×10^5	.003

U. S. GOVERNMENT PRINTING OFFICE: 1951

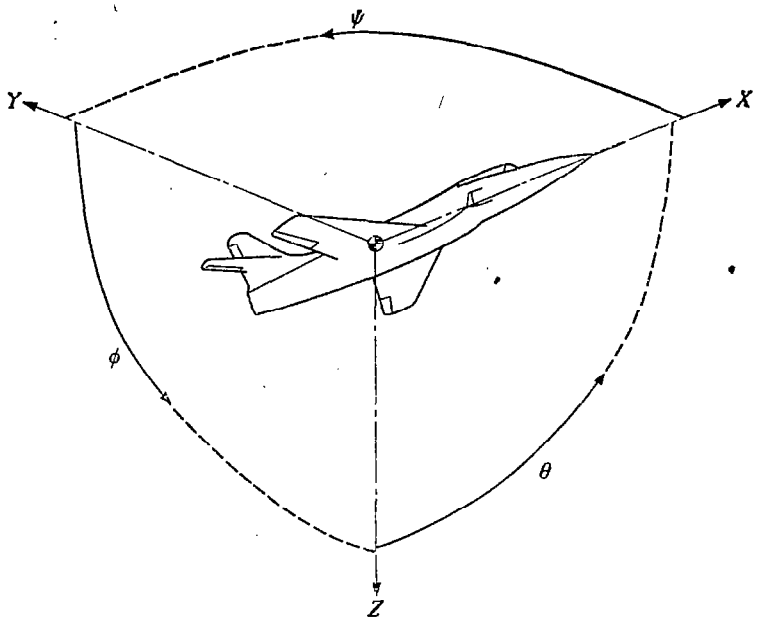

Positive directions of axes and angles (forces and moments) are shown by arrows

Axis		Force (parallel to axis) symbol	Moment about axis			Angle		Velocities	
Designation	Symbol		Designation	Symbol	Positive direction	Designation	Symbol	Linear (component along axis)	Angular
Longitudinal	X	X	Rolling	L	$Y \longrightarrow Z$	Roll	ϕ	u	p
Lateral	Y	Y	Pitching	M	$Z \longrightarrow X$	Pitch	θ	v	q
Normal	Z	Z	Yawing	N	$X \longrightarrow Y$	Yaw	ψ	w	r

Absolute coefficients of moment

$C_l = \frac{L}{qbS}$ (rolling) $\quad C_m = \frac{M}{qcS}$ (pitching) $\quad C_n = \frac{N}{qbS}$ (yawing)

Angle of set of control surface (relative to neutral position), δ. (Indicate surface by proper subscript.)

4. PROPELLER SYMBOLS

D Diameter

p Geometric pitch

p/D Pitch ratio

V' Inflow velocity

V_s Slipstream velocity

T Thrust, absolute coefficient $C_T = \frac{T}{\rho n^2 D^4}$

Q Torque, absolute coefficient $C_Q = \frac{Q}{\rho n^2 D^5}$

P Power, absolute coefficient $C_P = \frac{P}{\rho n^3 D^5}$

C_s Speed-power coefficient $= \sqrt[5]{\frac{\rho V^5}{P n^2}}$

η Efficiency

n Revolutions per second, rps

Φ Effective helix angle $= \tan^{-1}\left(\frac{V}{2\pi r n}\right)$

5. NUMERICAL RELATIONS

1 hp=76.04 kg-m/s=550 ft-lb/sec

1 metric horsepower=0.9863 hp

1 mph=0.4470 mps

1 mps=2.2369 mph

1 lb=0.4536 kg

1 kg=2.2046 lb

1 mi=1,609.35 m=5,280 ft

1 m=3.2808 ft